

Sparsity-Exploiting Channel Estimation For Unsourced Random Access With Fluid Antenna

Keru Zhou¹, Zhentian Zhang¹, Jian Dang^{1,2}, Qianqian Sun¹, Zaichen Zhang^{1,2}

¹National Mobile Communications Research Laboratory,

Frontiers Science Center for Mobile Information Communication and Security

Southeast University, Nanjing 210096, P. R. China

²Purple Mountain Laboratories, Nanjing 211111, P. R. China

Emails: {haibara, zhangzhentian, dangjian, sunqianqian, zczhang}@seu.edu.cn

Abstract—This work explores the channel estimation (CE) problem in uplink transmission for unsourced random access (URA) with a fluid antenna receiver. The additional spatial diversity in a fluid antenna system (FAS) addresses the needs of URA design in multiple-input and multiple-output (MIMO) systems. We present two CE strategies based on the activation of different FAS ports, namely alternate ports and partial ports CE. Both strategies facilitate the estimation of channel coefficients and angles of arrival (AoAs). Additionally, we discuss how to refine channel estimation by leveraging the sparsity of finite scatterers. Specifically, the proposed partial ports CE strategy is implemented using a regularized estimator, and we optimize the estimator’s parameter to achieve the desired AoA precision and refinement. Extensive numerical results demonstrate the feasibility of the proposed strategies, and a comparison with a conventional receiver using half-wavelength antennas highlights the promising future of integrating URA and FAS.

Index Terms—Channel estimation (CE), unsourced random access (URA), fluid antenna system (FAS).

I. INTRODUCTION

Unsourced random access (URA) techniques [1] address multiple access challenges in the context of massive machine-type communications with finite blocklengths. These techniques propose a potential multiple access code design to provide robust communication support. Significant degrees of freedom have been unlocked through its evolution towards a multiple-input and multiple-output (MIMO) system with multiple receiving antennas [2]. Recently, a novel MIMO system, the fluid antenna system (FAS), has garnered considerable attention due to its compelling features [3], [4], [5]. FAS offers additional spatial diversity with N position reconfigurable antennas or ports spaced linearly [6]. In comparison to conventional M -antenna maximum ratio combining systems, FAS achieves better outage probability performance with a sufficient number of ports. As a result, FAS channel reconstruction becomes essential for selecting the ports with the best channel gains [10].

Therefore, URA will naturally leverage the diversity gain generated by FAS, as the precision of channel estimation (CE) is pivotal for obtaining desirable decoding results at the MIMO URA receiver. Specifically, while URA often emphasizes promising concatenated encoder/decoder designs, the CE performance directly affects the performance of concatenated decoding under MIMO channels. Consequently, we investigate

potential CE strategies for FAS-URA in this paper. The main focuses of this paper are as follows:

1) *Channel Estimation For FAS-URA*: Under limited blocklengths and finite radio-frequency (RF) chains, we explain how to perform activity detection (AD) and estimate channel coefficients, considering the FAS planar geometric model in [11], which includes both scattered and line-of-sight (LOS) paths. We propose two strategies, namely alternate ports and partial ports CE, to facilitate these estimations. Additionally, we enable the estimation of arrival angles (AoAs) using a channel dictionary, exploiting the sparsity of finite scatterers.

2) *Partial Ports Estimation With Regularized Estimator*: We propose a regularized estimator for partial ports estimation, with or without prior knowledge of activity. Building on this regularized estimator, we further formulate the problem of port selection as an NP-hard problem with a feasible solution, providing guidance on how to achieve better AoA estimation.

3) *Comparison With Conventional Uniform Linear Array (ULA)*: Specifically, we compare the estimation performance between the proposed FAS-URA and the conventional ULA with the half-wavelength rule [12], [13], which has been widely considered in current URA designs [14], [15]. Numerical results demonstrate that the proposed CE via alternate ports provides better AoA precision, while the proposed CE via partial ports facilitates more accurate channel construction compared to the conventional ULA.

In the following, the system model for uplink FAS-URA is presented in Sec. II. In Sec. III, the proposed alternate ports CE is discussed. Sec. IV introduces the proposed AoA estimation using a channel dictionary, leveraging the sparsity of finite scatterers. In Sec. V, the proposed partial ports CE is detailed, along with the regularized estimator and the ports index selection optimization problem. Numerical results are provided in Sec. VI, and the conclusion is presented in Sec. VII.

II. URA WITH FLUID ANTENNA SYSTEM MODEL

A. Uplink Transmission Setups

We assume an uplink transmission with T_p duration where there are K_a single traditional antenna devices to be served by a receiver with a $W\lambda$ -wavelength fluid antenna. The fluid an-

tenna has N positions/ports to switch¹ and is connected to M RF-chains where normally $M \ll N$, i.e., only signals received from M ports connected to RF-chains can be de-mixed from analogue domain. Quasi-static fading without asynchronous error is considered in this work², i.e., the channel coefficients between devices and receiver retains unchanged during the transmission. For transmission in the URA [1], [2], the k -th device, $k \in [1 : K_a]$ uses B_p bits to select an L_p -length ($L_p \leq T_p$) pilot/codeword $\mathbf{x}_k \in \mathbb{C}^{L_p \times 1}$ from the common codebook $\mathbf{A} \in \mathbb{C}^{L_p \times 2^{B_p}}$ which can be generated from Gaussian signatures or sub-sampled DFT matrix [16]. And the pilot follows the power constraint of energy-per-bit under finite duration by $E_b/N_0 = (E_s T_p) / (B_p \sigma^2)$ where $\|\mathbf{x}_k\|_2^2 = E_s L_p$ and E_s is the unit power per channel uses.

B. Planar Propagation URA Channel Models: FAS vs ULA

For ease of description and the integrity of the content, we elaborate the geometric models of FAS and ULA under planar propagation³. FAS generates diversity by allowing the existence of multiple receiving points within fixed antenna length while the traditional ULA has a *half-wavelength* rule to follow. Thereupon, the following assumes both antennas have identical physical antenna size, i.e., $W\lambda = (M-1)\frac{\lambda}{2}$ with half-wavelength rule. Also, we consider transmission with finite L_s scatterers.

In Fig. 1, the planar propagation geometric model is depicted with finite scatterer paths and LOS path. The pivotal feature of FAS compared with traditional ULA is that the gap between N ports no longer follows the half-wavelength rule⁴, i.e., for ULA, the gap distance d between adjacent units equals to $d = \frac{\lambda}{2}$ while the gap distance is $d = \frac{W\lambda}{N-1}$ for FAS. Let \mathbf{g}_k denote the channel coefficient vector of the k -th device. However, both antennas always abide by identical physical size and share identical number of functional RF-chains.

For FAS⁵ channel [11] $\mathbf{g}_k = [g_{k,1}, g_{k,2}, \dots, g_{k,N}]^T \in \mathbb{C}^{N \times 1}$, element $g_{k,n}$, $n \in [1 : N]$ with the first port as benchmark can be expressed as:

$$g_{k,n} = \underbrace{\sigma_{k,0} e^{-j \frac{2\pi(n-1)W}{N-1} \cos \theta_{k,0}}}_{\text{LOS component}} + \underbrace{\sum_{l=1}^{L_s} \sigma_{k,l} e^{-j \frac{2\pi(n-1)W}{N-1} \cos \theta_{k,l}}}_{\text{scatterers component}}, \quad (1)$$

where Ω is the average energy of the channel, L_s is the number of scattered paths. For LOS component, $\sigma_{k,0} = \sqrt{\frac{K\Omega}{K+1}} e^{j\alpha_k}$, K is the Rice factor, α is the arbitrary LOS phase, and $\theta_{k,0}$ represents the azimuth AoA of the specular component of the

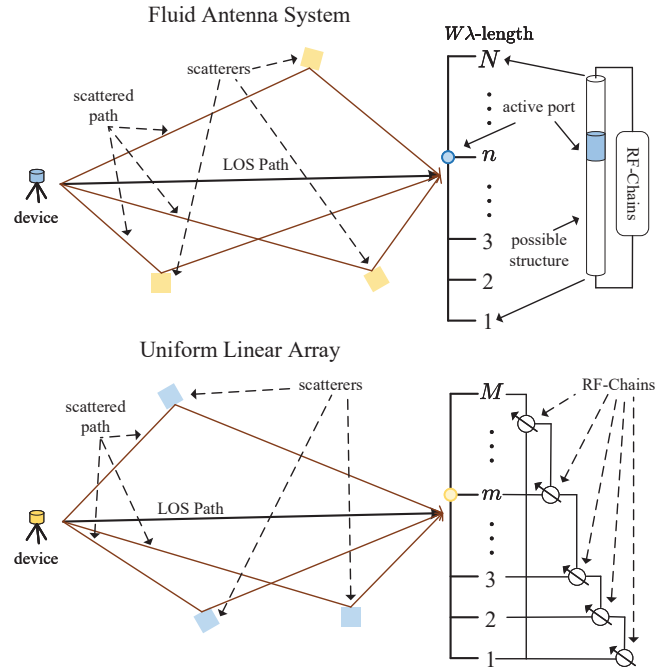


Fig. 1. Illustration of planar propagation with LOS path and multiple scattered paths under possible FAS and ULA structures. Only finite RF-chains are assumed, i.e., $M \ll N$.

k -th device. For scatterers component, $\sigma_{k,l}$ is the complex coefficient of the l -th path of the k -th device, $\theta_{k,l}$, $l \in [1 : L_s]$ represents the azimuth AoAs of the l -th path of k -th device, and $\sigma_{k,l}$ is the complex coefficient of the l -th path of k -th device satisfying $\sum_{l=1}^{L_s} |\sigma_{k,l}|^2 = \frac{\Omega}{K+1}$. Moreover, for the traditional ULA geometric model [12], [13], $\mathbf{g}_k = [g_{k,1}, g_{k,2}, \dots, g_{k,M}]^T \in \mathbb{C}^{M \times 1}$, element $g_{k,m}$, $m \in [1 : M]$ can be expressed as

$$g_{k,m} = \underbrace{\sigma_{k,0} e^{-j \frac{2\pi(m-1)d}{\lambda} \cos \theta_{k,0}}}_{\text{LOS component}} + \underbrace{\sum_{l=1}^{L_s} \sigma_{k,l} e^{-j \frac{2\pi(m-1)d}{\lambda} \cos \theta_{k,l}}}_{\text{scatterers component}}, \quad (2)$$

where only the spatial response part $e^{-j \frac{2\pi(m-1)d}{\lambda} \cos \theta_{k,l}}$ is different from FAS and others share identical physical representations in (1). Yet, we have to note that there is no way the FAS receiver can observe decoupled signals from all N ports simultaneously due to the limited RF-chains $M \ll N$. And we have made fair assumptions including the length of antenna and the number of RF-chains. In the sequel, the work is established on the justified assumptions with adequate equity.

III. ALTERNATE PORTS CHANNEL ESTIMATION

Reminding that only M ports can be activated simultaneously, however, the receiver can make proper ports selection only with knowledge of all channel coefficients between ports and devices. Based on this observation, an alternate ports channel estimation (AP-CE) strategy is proposed for FA-URA. Specifically, AP-CE receives pilot signals from different sets of ports in each duration of time while switching different sets

¹The potential switching delay becomes negligible with advances in antenna designs and novel materials [3], [7], [8].

²All works in this paper is readily applicable under scenario with large fading effect considering path loss.

³Near-filed problem is not considered in this work.

⁴This means there will be many correlated ports in vicinity, which however introduces more degree-of-freedom. Please refer to [9], [10] for more detail.

⁵Fig. 1 is an abstract illustration of the FA structure which does not imply any specific implementation method. It could be realized by metamaterial or reconfigurable pixel designs if fast switching speed is required. Also, a two port configuration for FA is also possible.

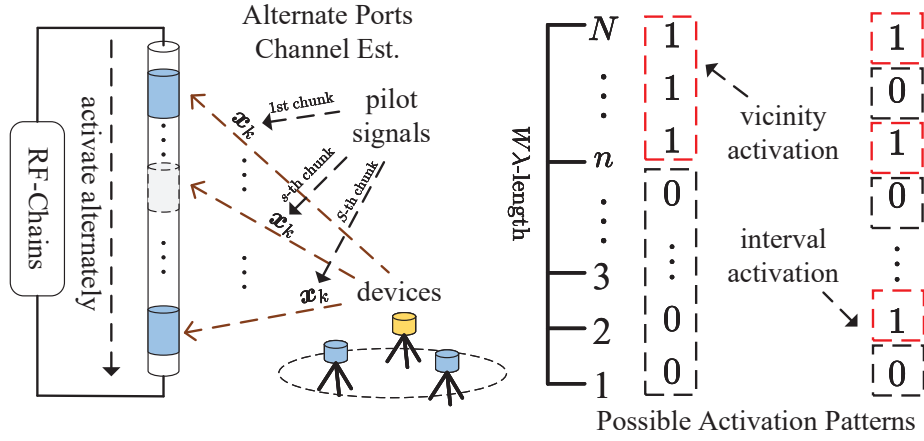


Fig. 2. Illustration of the proposed AP-CE strategy and possible ports activation patterns (vicinity/interval activation).

of ports to be activated. In this way, the receiver can observe the channel condition of all ports. In Fig. 2, we illustrate the proposed AP-CE strategy and give examples on possible ports activation patterns including activating sets of ports in vicinity or ports in interval gaps every switch time.

Let $N_{obs}, N_{obs} \leq M$ denote the number of ports activated/observed by the receiver. Therefore, there are $S = N/N_{obs}$ sets of ports to be estimated and the duration for CSI estimation is also split into S chunks with channel uses $T_p = SL_p$. The channel vector between the k -th device and all ports based on model in (1) can be written as:

$$\mathbf{g}_k = \begin{bmatrix} g_{k,1} \\ g_{k,2} \\ g_{k,3} \\ \vdots \\ g_{k,n} \\ \vdots \\ g_{k,N} \end{bmatrix} = \begin{bmatrix} \mathbf{g}_{k,1} \\ \mathbf{g}_{k,2} \\ \vdots \\ \mathbf{g}_{k,s} \\ \vdots \\ \mathbf{g}_{k,S} \end{bmatrix}, \quad \mathbf{g}_{k,s} = \begin{bmatrix} g_{k,(1+(s-1)N_{obs})} \\ g_{k,(2+(s-1)N_{obs})} \\ g_{k,(3+(s-1)N_{obs})} \\ \vdots \\ g_{k,(sN_{obs})} \end{bmatrix}, \quad (3)$$

where $\mathbf{g}_{k,s} \in \mathbb{C}^{N_{obs} \times 1}$ is the channel coefficient between the activated ports and k -th device at the s -th chunk of duration time where there are N_{obs} elements to be estimated. During each chunk of duration, the received signal $\mathbf{Y}_{p,s} \in \mathbb{C}^{L_p \times N_{obs}}$ can be written as:

$$\mathbf{Y}_{p,s} = \sum_k \mathbf{x}_k \mathbf{g}_{k,s}^T + \mathbf{N}_s, \quad s \in [1:S], \quad (4)$$

where \mathbf{N}_s is the additive white Gaussian noise (AWGN) following distribution of $\mathcal{CN}(\mathbf{0}, \sigma^2 \mathbf{I})$ with zero mean and σ^2 variance. Therefore, the total signals $\mathbf{Y}_p \in \mathbb{C}^{L_p \times N}$ received in T_p duration is

$$\begin{aligned} \mathbf{Y}_p &= \underbrace{[\mathbf{Y}_{p,1}, \mathbf{Y}_{p,2}, \dots, \mathbf{Y}_{p,S}]}_{S \text{ chunks}} \\ &= \sum_k \mathbf{x}_k^p \mathbf{g}_k^T + \mathbf{N} = \mathbf{A}\mathbf{G} + \mathbf{N}, \end{aligned} \quad (5)$$

where \mathbf{N} represents AWGN, $\mathbf{G} \in \mathbb{C}^{2^{B_p} \times N}$ is a row-sparse matrix with only nonzero elements in K_a rows and others all

zeros and \mathbf{A} is the common codebook. Thus, the joint AD and CE problem in (5) is formulated into a sparse recovery problem.

However, we have to note that model in (5) is distinctive to the common linear model under conventional ULA channel which is normally in the form of $\mathbf{Y} = \mathbf{A}\mathbf{H} + \mathbf{N}$ where $\mathbf{H} \in \mathbb{C}^{2^{B_p} \times M}$. Since ULA has M antenna unit all connected to RF-chains, the receiver with ULA antenna can receive decoupled signals from all M unit throughout the T_p duration, i.e., $L_p = T_p$ while for the proposed AP-CE, $L_p = T_p/N$ and $M \ll N$. Though the pilot length is shortened in FA-URA, the diversity of antenna is increased under FA-URA. We solve this sparse recovery problem following the spirit of simultaneous orthogonal matching pursuit (SOMP) [17]. We summarize the SOMP in Algorithm 1. SOMP is a greedy iterative algorithm

Algorithm 1: AP-CE By SOMP

- Input:** Signal \mathbf{Y}_p , common codebook \mathbf{A}
Output: Active Indices and Estimated Channel Vectors
- 1 Initialization: $k \leftarrow 0$, residual $\mathbf{R} \leftarrow \mathbf{Y}_p$, $\mathcal{S} \leftarrow \emptyset$, $\mathbf{G} \leftarrow \mathbf{0}$;
 - 2 **while** $k \leq \tilde{K}_a$ **do**
 - 3 $i \leftarrow \arg \max_{i_k^p \in \{1, 2, \dots, 2^{B_p}\}} \|\mathbf{R}^H \mathbf{A}(:, i_k^p)\|_2 / \|\mathbf{A}(:, i_k^p)\|_2$;
 - 4 Activity Support $\mathcal{S} \leftarrow \mathcal{S} \cup i$;
 - 5 Projection Span Space $\Phi \leftarrow \mathbf{A}(:, \{\mathcal{S}\})$;
 - 6 Update residual $\mathbf{R} \leftarrow (\mathbf{R} - \Phi \Phi^\dagger \mathbf{Y}_p)$ and $(\cdot)^\dagger$ denotes Moore-Penrose inverse;
 - 7 $k \leftarrow k + 1$;
 - 8 **end**
 - 9 Active support \mathcal{S} and channel estimation
- $$\{\tilde{\mathbf{g}}_k\} \leftarrow (\mathbf{A}(:, \{\mathcal{S}\})^H \mathbf{A}(:, \{\mathcal{S}\}))^{-1} \mathbf{A}(:, \{\mathcal{S}\})^H \mathbf{Y}_p.$$
-

to solve sparse recovery problems. SOMP algorithm selects the column of the measurement matrix with the maximum correlation between the current residual at each iteration and adds its index to the output list. The complexity of SOMP

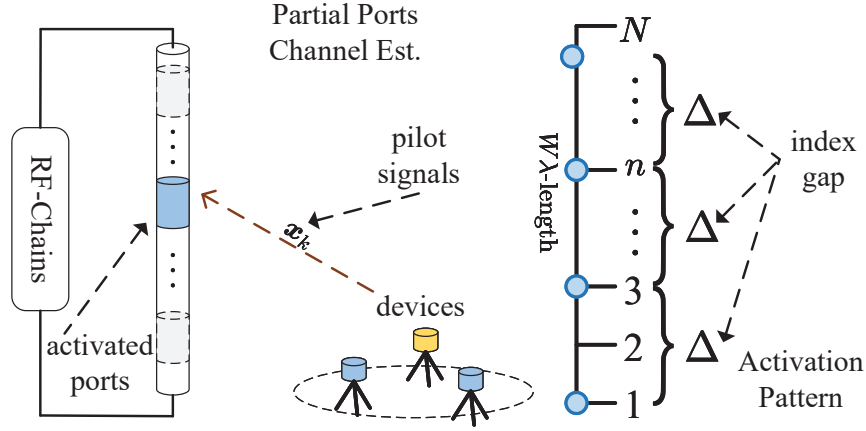


Fig. 3. Illustration of the proposed PP-CE strategy and ports activation patterns with index gap Δ .

is dominated by the Moore-Penrose inverse at each iteration, scaling as $\mathcal{O}(NL_p^3)$. Meanwhile, the line 2 of SOMP algorithm requires the number of activity which can be estimated by the power information of the received signal:

$$\tilde{K}_a = \left\lfloor \frac{1}{E_s L_p} \left(\frac{\|\mathbf{Y}_p\|_F^2}{N\Omega} - \sigma^2 L_p \right) \right\rfloor. \quad (6)$$

IV. AOA ESTIMATION AND CHANNEL REFINEMENT

In accordance with model (1) and (3), it is possible to estimate AoAs and even the complex coefficients of the propagation paths, which is often known as channel reconstruction. Let I_a denote the number of AoA samples and is adequate large for certain AoA resolution. One can form a channel dictionary based on (1). The normalized ports response vector $\mathbf{d}_i \in \mathbb{C}^{N \times 1}$ at the receiver can be written as:

$$\mathbf{d}_i = \frac{1}{\sqrt{N_{obs}}} \left[1, e^{-j\frac{2\pi W}{N-1} \cos \theta_i}, \dots, e^{-j\frac{2\pi(n-1)W}{N-1} \cos \theta_i}, \dots \right]^T \quad (7)$$

where $\theta_i, i \in [1 : I_a]$ is the AoA sample, for alternate ports estimation $N_{obs} = N$, for partial ports estimation, $N_{obs} = M$. Therefore, one can obtain a prescribed channel response dictionary $\mathbf{D} = [\mathbf{d}_1, \mathbf{d}_2, \dots, \mathbf{d}_{I_a}] \in \mathbb{C}^{N \times I_a}$. Meanwhile, considering there are $(L_s + 1)$ propagation paths (if LOS is considered), we can write (1) in a compact form:

$$\begin{aligned} \mathbf{g}_k &= \sum_{l=0}^{L_s} \sigma_{k,l} \mathbf{d}_l \\ &= \underbrace{[\mathbf{d}_0 \quad \dots \quad \mathbf{d}_l \quad \dots \quad \mathbf{d}_{L_s}]}_{\text{ports response}} \underbrace{\begin{bmatrix} \sigma_{k,0} \\ \vdots \\ \sigma_{k,l} \\ \vdots \\ \sigma_{k,L_s} \end{bmatrix}}_{\text{path coefficients}} = \mathbf{D} \boldsymbol{\sigma}_k, \quad (8) \end{aligned}$$

where $\boldsymbol{\sigma}_k \in \mathbb{C}^{I_a \times 1}$ is an $(L_s + 1)$ -sparse vector denoting the path coefficient vector. Thus, AoA estimation is also converted into a sparse recovery problem. We note that the SOMP is

also applicable for model (8). The estimated channel vectors by Algorithm 1 can be refined by the AoA dictionary.

V. PARTIAL PORTS CHANNEL ESTIMATION

Another plausible way is only observing signals from $N_{obs} \leq M$ ports within the T_p duration, i.e., the length of pilot is $L_p = T_p$ and no longer shortened which is called as partial ports channel estimation (PP-CE). Therefore, the received signal model resembles (5) except for that $\mathbf{Y}_p \in \mathbb{C}^{T_p \times N_{obs}}$, $\mathbf{A} \in \mathbb{C}^{T_p \times 2^{B_p}}$, $\mathbf{G} \in \mathbb{C}^{2^{B_p} \times N_{obs}}$. We illustrate the PP-CE in Fig. 3. The pilot transmission is no longer split into chunks. The aforementioned methods in Sec. III and IV can be still utilized to conduct AD, CE and AoA estimation. However, in order to reconstruct the channel from partially observed ports. The receiver needs to select good ports to be observed. The following elaborates how to choose good Δ .

Assuming ports are observed from the 1st port with index gap Δ . Based on (7),(8), the coefficient of the observed ports can be expressed as:

$$\begin{aligned} \mathbf{g}_k &= \begin{bmatrix} g_{k,1} \\ g_{k,2} \\ \vdots \\ g_{k,N_{obs}} \end{bmatrix} = \begin{bmatrix} \sum_{l=0}^{L_s} \sigma_{k,l} e^{-j\frac{2\pi \Delta W}{N-1} \cos \theta_{k,l}} \\ \vdots \\ \sum_{l=0}^{L_s} \sigma_{k,l} e^{-j\frac{2\pi N_{obs} \Delta W}{N-1} \cos \theta_{k,l}} \end{bmatrix} = \\ &= \underbrace{\begin{bmatrix} 1 & \dots & 1 \\ e^{-j\frac{2\pi \Delta W}{N-1} \cos \theta_{k,0}} & \dots & e^{-j\frac{2\pi \Delta W}{N-1} \cos \theta_{k,L_s}} \\ \vdots & \ddots & \vdots \\ e^{-j\frac{2\pi \Delta N_{obs} W}{N-1} \cos \theta_{k,0}} & \dots & e^{-j\frac{2\pi \Delta N_{obs} W}{N-1} \cos \theta_{k,L_s}} \end{bmatrix}}_{\mathbf{W} \boldsymbol{\sigma}_k} \begin{bmatrix} \sigma_{k,0} \\ \sigma_{k,1} \\ \vdots \\ \sigma_{k,L_s} \end{bmatrix}, \quad (9) \end{aligned}$$

where $\mathbf{W} \in \mathbb{C}^{N_{obs} \times (L_s + 1)}$ is a Vandermonde matrix with Δ as parameter to be optimized. Moreover, it requires $N_{obs} \geq L_s + 1$ to estimate the path coefficients. Without loss of generality, the relationship between path coefficients and the estimated channel is $\hat{\mathbf{g}}_k = \mathbf{W} \boldsymbol{\sigma}_k + \mathbf{n}_k$ where \mathbf{n}_k is noisy derivations

with variance σ_d^2 . The goal is to obtain the path coefficients with minimum deviation, we form the subject goal as:

$$\arg \min_{\sigma_k} \|\tilde{\mathbf{g}}_k - \mathbf{W}\sigma_k\|_2^2 + \underbrace{\frac{(K+1)\alpha}{\Omega} \|\sigma_k\|_2^2}_{\text{regularizer with } \gamma = \frac{(K+1)\alpha}{\Omega}}, \quad (10)$$

where the regularizer is considered due to aggregate path coefficient power in (1) and regularization constant is flexibly parameterized. The target function can be formulated as:

$$\begin{aligned} & \|\tilde{\mathbf{g}}_k - \mathbf{W}\sigma_k\|_2^2 + \gamma \|\sigma_k\|_2^2 \\ &= (\tilde{\mathbf{g}}_k - \mathbf{W}\sigma_k)^H (\tilde{\mathbf{g}}_k - \mathbf{W}\sigma_k) + \gamma \sigma_k^H \sigma_k \\ &= \tilde{\mathbf{g}}^H \tilde{\mathbf{g}} - \tilde{\mathbf{g}}^H \mathbf{W}\sigma_k - \sigma_k^H \mathbf{W}^H \tilde{\mathbf{g}} + \sigma_k^H \mathbf{W}^H \mathbf{W}\sigma_k + \gamma \sigma_k^H \sigma_k, \end{aligned} \quad (11)$$

whose gradient by σ_k can be calculated as

$$\nabla_{\sigma^2} = -2\mathbf{W}^H \tilde{\mathbf{g}}_k + 2\mathbf{W}^H \mathbf{W}\sigma_k + 2\gamma \sigma_k, \quad (12)$$

and by setting $\nabla_{\sigma^2} = 0$, the solution of (10) is:

$$\tilde{\sigma}_k = (\mathbf{W}^H \mathbf{W} + \gamma \mathbf{I})^{-1} \mathbf{W}^H \tilde{\mathbf{g}}_k, \quad (13)$$

where \mathbf{I} is the unit matrix. With activity results, one can estimate channels by (13) with regularized estimator. Subsequently, the goal is to find out Δ producing lowest estimation error, the deviation of path coefficients can be expressed as:

$$\begin{aligned} & \arg \min_{\Delta} \|\tilde{\sigma}_k - \sigma_k\|_2^2 \\ & \text{subject to } \Delta \in \mathcal{N}_0 = \{1, 2, \dots, \frac{N}{M}\}, \end{aligned} \quad (14)$$

Substitute (9) into (14), we have:

$$\begin{aligned} & \|\tilde{\sigma}_k - \sigma_k\|_2^2 \\ &= \|(\mathbf{W}^H \mathbf{W} + \gamma \mathbf{I})^{-1} \mathbf{W}^H (\tilde{\mathbf{g}}_k - \mathbf{g}_k)\|_2^2 \\ &= \|(\mathbf{W}^H \mathbf{W} + \gamma \mathbf{I})^{-1} \mathbf{W}^H \mathbf{n}_k\|_2^2 \end{aligned} \quad (15)$$

By singular value decomposition, we have decomposed matrix $\mathbf{W} = \mathbf{U}\Sigma\mathbf{V}^H$ where \mathbf{U}, \mathbf{V} are unitary matrices and unitary matrix has favourable features such as $\mathbf{U}^H \mathbf{U} = \mathbf{I}$, $\mathbf{U}^H = \mathbf{U}^{-1}$, and $\|\mathbf{U}\mathbf{x}\|_2^2 = \|\mathbf{x}\|_2^2$. Substitute decomposed \mathbf{W} into (15):

$$\begin{aligned} & \|(\mathbf{W}^H \mathbf{W} + \gamma \mathbf{I})^{-1} \mathbf{W}^H \mathbf{n}_k\|_2^2 \\ &= \|((\mathbf{V}\Sigma^H \mathbf{U}^H)(\mathbf{U}\Sigma\mathbf{V}^H) + \gamma \mathbf{I})^{-1} (\mathbf{V}\Sigma^H \mathbf{U}^H) \mathbf{n}_k\|_2^2 \\ &= \|(\mathbf{V}\Sigma^H \Sigma \mathbf{V}^H + \gamma \mathbf{V}\mathbf{V}^H)^{-1} (\mathbf{V}\Sigma^H \mathbf{U}^H) \mathbf{n}_k\|_2^2 \\ &= \|(\Sigma^H \Sigma + \gamma \mathbf{I})^{-1} \Sigma^H \mathbf{n}_k\|_2^2 \\ &\approx \sigma_c^2 \text{Tr} \left[((\Sigma^H \Sigma + \gamma \mathbf{I})^{-1} \Sigma^H)^2 \right] \end{aligned} \quad (16)$$

where $\text{Tr}[\cdot]$ denotes the trace of the matrix. Hereafter, the problem in (14) is now equivalent to:

$$\begin{aligned} & \arg \min_{\Delta} \text{Tr} \left[((\Sigma^H \Sigma + \gamma \mathbf{I})^{-1} \Sigma^H)^2 \right] \\ & \text{subject to } \Delta \in \mathcal{N}_0 = \{1, \dots, \frac{N}{M}\}, \end{aligned} \quad (17)$$

which is an NP-hard problem. However, we can solve this problem via exhaust search since $|\mathcal{N}_0| = \frac{N}{M} \ll N$ with maximum complexity $\mathcal{O}(\frac{N}{M})$.

VI. NUMERICAL RESULTS

In this section, we illustrate the results of the proposed AP-CE and the proposed PP-CE with regularized estimator. We compare the results with URA CE under ULA model. Universal parameters are $K_a = 5$, amount of finite scatters $L_s = 3$, $T_p = 200$, Rive factor $K = 2$, $\Omega = 1$, number of AoA samples $I_a = 100$, number of RF-chains and ports $M = 10$ and $N = 100$. For AP-CE, $N_{obs} = N$ and for PP-CE, $N_{obs} = M$. The averaged normalized mean square error (NMSE) of CE is defined by $\mathbb{E}\{\|\mathbf{g}_k - \tilde{\mathbf{g}}_k\|_2^2\} / \mathbb{E}\{\|\mathbf{g}_k\|_2^2\}$ and the precision of AoA estimation is denoted by AoA NMSE $\mathbb{E}\{|\theta_{k,l} - \tilde{\theta}_{k,l}|\} / \mathbb{E}\{|\theta_{k,l}|\}$. If K_a is known, the AD error consists of only error of missed detection otherwise AD error is the summation of error of missed detection and false alarm. Only those correctly detected are used to calculate the corresponding NMSE.

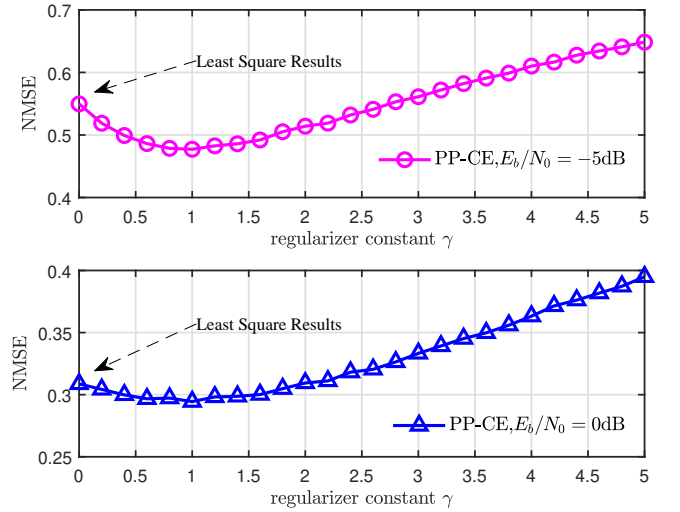


Fig. 4. Performance with different power allocation under geometric model.

1) *PP-CE Parameter Setups γ and Δ* : We illustrate the performance of the proposed PP-CE with different regularizer γ and the value of (17) for justified parameter setups. Firstly, we illustrate the channel NMSE versus γ with $\Delta = 10$ in Fig. 4. The viability of the proposed regularized CE is validated compared with the results under $\gamma = 0$ which the least square-oriented estimation referred in [10]. Improved CE can be observed and the following simulations are conducted with $\gamma = 1$.

Secondly, we illustrate the value of target function $\text{Tr} \left[((\Sigma^H \Sigma + \gamma \mathbf{I})^{-1} \Sigma^H)^2 \right]$ under different Δ to determine good index gap option. Fig. 5 depicts the subsection function value versus different Δ and N with $E_b/N_0 = 0\text{dB}$. In the sequel, index gap is fixed to $\Delta = 10$. To further validate the effectiveness of the proposed gap selection strategy, we illustrate the AoA NMSE versus different Δ in Fig. 6. Similar tenancy can be observed in Fig. 5 and 6 indicating the viability of the proposed selection strategy.

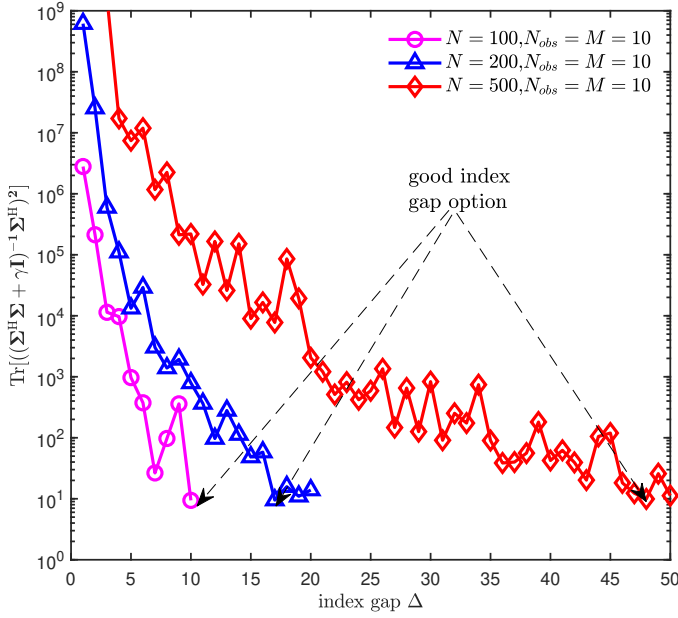


Fig. 5. The value of subject function (17) under different index gaps and number of ports.

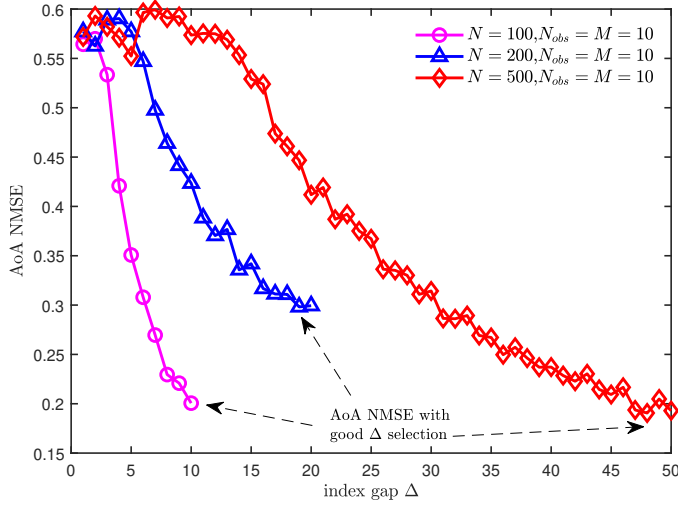


Fig. 6. Performance of AoA estimation of PP-CE versus index gap under different N and $E_b/N_0 = 0\text{dB}$.

2) *AD and AoA Estimation*: We illustrate the performance of AD and AoA estimation with K_a prior and with estimated \hat{K}_a by (6) under different estimation strategy and channel model in Fig. 7 with different energy-per-bit. Overall, the precision of estimation drops with the increased energy-per-bit. Moreover, the proposed PP-CE shows the best performance among all in terms of AD error and AoA NMSE. It indicates that FAS-URA has potential to obtain enhanced estimation capability compared with conventional ULA channel model. Notably, though the proposed AP-CE only utilizes shortened pilot, it has much better AoA estimation performance compared with ULA model. It means the proposed AP-CE has more superiority in scenario where AoA estimation matters.

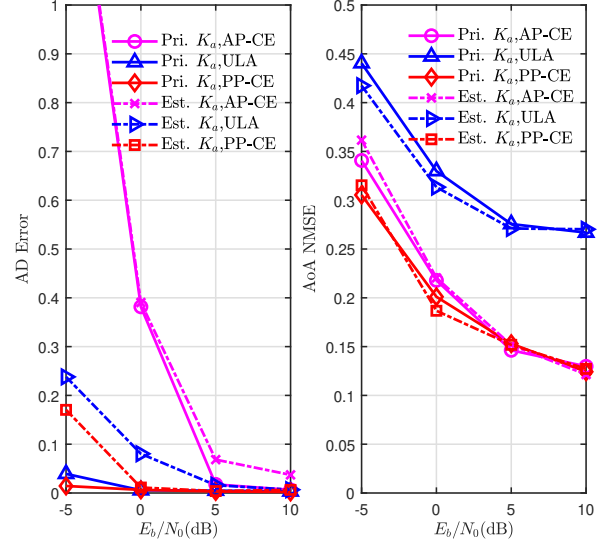


Fig. 7. Performance of AD And AoA NMSE with/without activity prior.

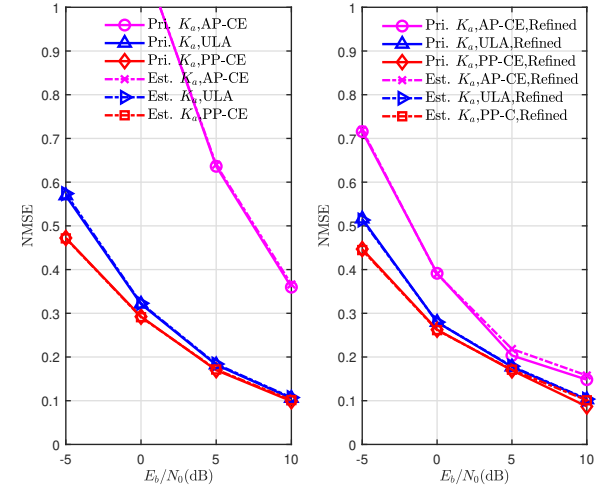


Fig. 8. Performance of CE with refinement with/without activity prior.

3) *CE and Estimation Refinement*: Furthermore, we compare the performance of CE with refinement via geometric models of FAS and ULA. Overall, the proposed PP-CE has the best CE performance compared with others with or without estimation refinement by channel dictionary. Notably, CE refinement can drastically improve the performance of the proposed AP-CE. Meanwhile, the prior of activity does not generate much derivation for CE under all strategies or models. We also investigate the impact from LOS path with different Rice factor with $E_b/N_0 = 0\text{dB}$. The results demonstrate that the proposed schemes can well tackle CE under different Rice factor.

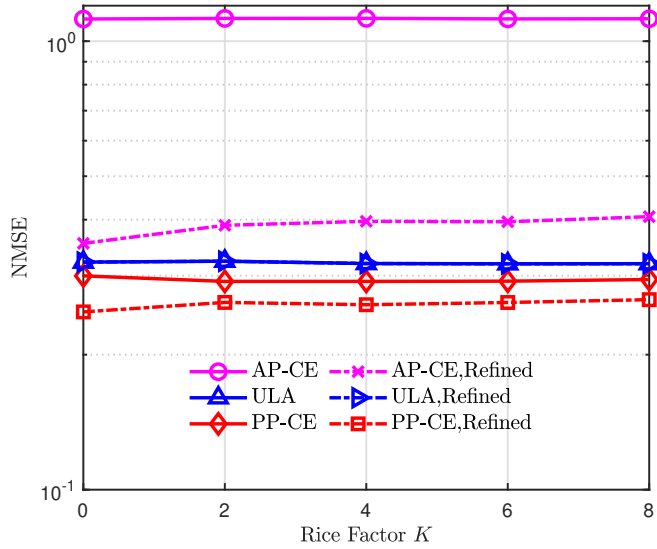


Fig. 9. Performance of CE versus different Rice factor with $E_b/N_0 = 0\text{dB}$.

VII. CONCLUSION

In this work, we investigate the CE problem for URA with fluid antennas. Channel coefficient and AoA estimation are enabled through different strategies, namely alternate/partial ports CE, by exploiting the sparsity of finite scatterers. In particular, a regularized estimator for partial ports CE is developed, with an optimized port index gap, to achieve desirable AoA estimation and improved channel refinement. Numerical results highlight the promising potential of the FAS-URA. Future work will address concatenated decoding, considering FAS diversity.

ACKNOWLEDGMENT

This work is supported by NSFC projects (61971136, 61960206005), the Fundamental Research Funds for the Central Universities (2242022k60001, 2242021R41149, 2242023K5003).

REFERENCES

- [1] Y. Wu, X. Gao, S. Zhou, W. Yang, Y. Polyanskiy and G. Caire, "Massive access for future wireless communication systems," *IEEE Wireless Commun.*, vol. 27, no. 4, pp. 148-156, Aug. 2020.
- [2] Y. Li, J. Dai, Z. Si and et al., "Unsourced multiple access for 6G massive machine type communications," *China Commun.*, vol. 19, no. 3, pp. 70-87, Mar. 2022.
- [3] K. -K. Wong, A. Shojaefard, K. -F. Tong and Y. Zhang, "Fluid antenna systems," *IEEE Trans. Wireless Commun.*, vol. 20, no. 3, pp. 1950-1962, March 2021.
- [4] C. Psomas, P. J. Smith, H. A. Suraweera and I. Krikidis, "Continuous fluid antenna systems: Modeling and analysis," *IEEE Commun. Lett.*, vol. 27, no. 12, pp. 3370-3374, Dec. 2023.
- [5] M. Khammassi, A. Kammoun and M.-S. Alouini, "A new analytical approximation of the fluid antenna system channel," *IEEE Trans. Wireless Commun.*, vol. 22, no. 12, pp. 8843-8858, Dec. 2023.
- [6] W. K. New, K. K. Wong, H. Xu, K. F. Tong and C.-B. Chae, "An information-theoretic characterization of MIMO-FAS: Optimization, diversity-multiplexing tradeoff and q -outage capacity," *IEEE Trans. Wireless Commun.*, vol. 23, no. 6, pp. 5541-5556, Jun. 2024.
- [7] K. K. Wong and K. F. Tong, "Fluid antenna multiple access," *IEEE Trans. Wireless Commun.*, vol. 21, no. 7, pp. 4801-4815, Jul. 2022.
- [8] K. K. Wong, K. F. Tong, Y. Chen and Y. Zhang, "Fast fluid antenna multiple access enabling massive connectivity," *IEEE Commun. Lett.*, vol. 27, no. 2, pp. 711-715, Feb. 2023.
- [9] K. K. Wong, D. Morales-Jimenez, K. F. Tong and C.-B. Chae, "Slow fluid antenna multiple access," *IEEE Trans. Commun.*, vol. 71, no. 5, pp. 2831-2846, May 2023.
- [10] W. K. New *et al.*, "A tutorial on fluid antenna system for 6G networks: Encompassing communication theory, optimization methods and hardware designs," *IEEE Commun. Surv. Tutor.*, Early Access, doi: 10.1109/COMST.2024.3498855, 2024.
- [11] K.-K. Wong, K.-F. Tong, Y. Chen, and Y. Zhang, "Extra-large MIMO enabling slow fluid antenna massive access for millimeter-wave bands," *Electronics Letters*, vol. 58, no. 25, pp. 1016-1018, 2022.
- [12] J. Liu and X. Wang, "Sparsity-exploiting blind receiver algorithms for unsourced multiple access in MIMO and massive MIMO channels," *IEEE Trans. Commun.*, vol. 69, no. 12, pp. 8055-8067, Dec. 2021.
- [13] H. Chu, L. Zheng and X. Wang, "Super-resolution mmWave channel estimation for generalized spatial modulation systems," *IEEE J. Sel. Topics Signal Process.*, vol. 13, no. 6, pp. 1336-1347, Oct. 2019.
- [14] Z. Zhang, *et al.*, "Efficient ODMA for unsourced random access in MIMO and hybrid massive MIMO," *IEEE Internet Things J.*, vol. 11, no. 23, pp. 38846-38860, 1 Dec.1, 2024.
- [15] J. Liu and X. Wang, "Sparsity-exploiting blind receiver algorithms for unsourced multiple access in MIMO and massive MIMO channels," *IEEE Trans. Commun.*, vol. 69, no. 12, pp. 8055-8067, Dec. 2021.
- [16] A. Fengler, O. Musa, P. Jung, and G. Caire, "Pilot-based unsourced random access with a massive MIMO receiver, interference cancellation, and power control," *IEEE J. Sel. Areas Commun.*, vol. 40, no. 5, pp. 1522-1534, May 2022.
- [17] J. -F. Determe, J. Louveaux, L. Jacques and F. Horlin, "On the exact recovery condition of simultaneous orthogonal matching pursuit," *IEEE Signal Process. Lett.*, vol. 23, no. 1, pp. 164-168, Jan. 2016.